Physica Scripta. Vol. T8, 77–83, 1984

Lifetime Measurements in Highly Ionised Atoms

L. J. Curtis

Department of Physics and Astronomy, The University of Toledo, Toledo, Ohio 43606, U.S.A.

Received August 19, 1983; accepted September 20, 1983

Abstract

Recent developments in the measurement of lifetimes of excited states in highly ionised atoms using fast ion beam excitation methods are reviewed. The applicability and precision of these methods are discussed in the context of specific measurements and compared with existing theoretical capabilities.

1. Introduction

Despite many recent technical advances in the study of neutral and few times ionised systems, the only generally applicable method for direct measurement of lifetimes in highly ionised atoms is through in-flight excitation of a fast ion beam by a thin foil. The method has many applications in addition to lifetime measurements and a rich literature on this subject exists. Comprehensive descriptions and bibliographic references can be found in several recent reviews [1–3].

Foil excitation of a fast ion beam provides access to nearly any ionisation stage of any atom, although not all excited states within a given ion are amenable to lifetime determinations. The high density excitation conditions in the foil cause a large fraction of the beam particles to be excited and produce copious multiple electron excitation, but also lead to non-selective excitation with associated problems of cascading and blending. The low density decay conditions insure that there is no radiation trapping or collisional transfer, that high n and l states are not Stark quenched or broadened, and that metastable states have time to decay spontaneously. However, the low density also means that detection levels are low. Measurements of emitted intensity as a function of time since excitation can be made by detection of photons or autoionising electrons [4] at a variable distance downstream from the foil.

In the past several years many improvements have been made in the wavelength and time resolution of this method. Optical techniques [6] that exploit the angular Doppler dispersion to narrow and enhance spectral lines can yield wavelength accuracies of 50 mÅ [5]. Picosecond time resolution has been obtained through optical and mechanical systems that can reproducibly view a beam segment shorter than 0.1 mm.

The use of this method to determine lifetimes does have limitations, imposed by the narrow adjustability of the time-of-flight window, the efficiencies of the detectors in the various wavelength regions, and the blending and cascading conditions of the level studied. Isoelectronic plots of lifetime versus wavelength for several ground state transitions that have been seen in tokamak spectra are given in Fig. 1, which illustrate some of these limitations. Curve (a) is the $4s\ ^2S_{1/2}$–$4p\ ^2P_{3/2}$ resonance transition in the Cu sequence [7], which has a decay length long enough to be measurable [8, 9] for ions up to approximately W^{+45}. Curve (b) is the $2s^2\ ^1S_0$–$2s2p\ ^3P_1$ intercombination line in the Be sequence [10], which has a decay length short enough to be measured [11, 12] only at high stages of ionisation.

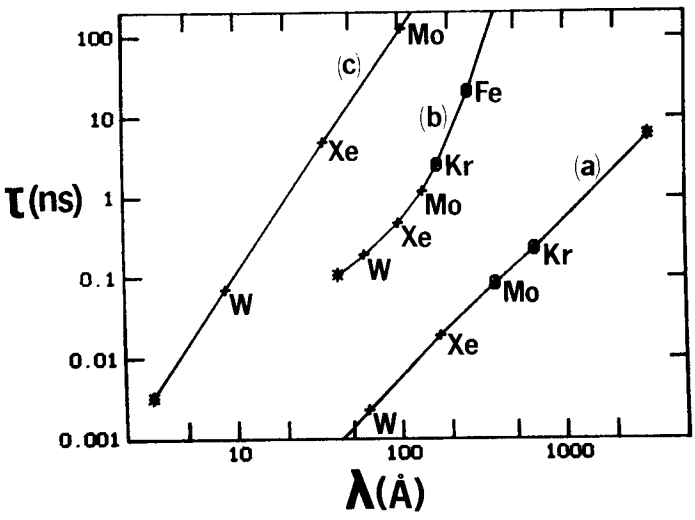

Fig. 1. Isoelectronic loci of lifetime vs. wavelength: (a) $4s\ ^2S_{1/2}$–$4p\ ^2P_{3/2}$ transition in the Cu sequence; (b) $2s^2\ ^1S_0$–$2s2p\ ^3P_1$ transition in the Be sequence; (c) $2p\ ^2P_{1/2}$–$2p\ ^2P_{3/2}$ transition in the B sequence. Solid lines trace theoretical calculations, (○) denotes each measured value, (+) labels specific ions and (★) denotes an end of a sequence. Theoretical and experimental values are from (a) [7–9], (b) [10–12] and (c) eqs. (1) and (2).

Curve (c) is the M1 $2p\ ^2P_{1/2}$–$2p\ ^2P_{3/2}$ fine structure transition in the ground state term of the B sequence, which has a narrow range of ions for which its decay length is neither too long nor its wavelength too short for measurement.

If accepted procedures are followed to remove blends, account for cascades, achieve sufficient statistical accuracy, etc., accuracies of lifetime measurements are typically 2–8%. Although higher accuracies can be achieved in favourable cases [13] and lower accuracies are sometimes accepted in unfavourable but interesting cases, most reported measurements quote accuracies within this range. It is therefore important to match this accuracy with the theoretical or applicational requirements. A number of specific examples will be discussed below.

2. Forbidden or inhibited transitions

There has been much discussion of the effects of blending and cascading on lifetime measurements. Certainly blending can be minimised by high spectral resolution and cascades can be accounted for by the joint measurement of all associated decay curves. However, there are cases where cascading becomes an advantage, causing lines that would be weak in absorption or selectively-populated emission to become strong. This is the case for low-lying forbidden or inhibited transitions, which become heavily populated due to shorter-lived cascading. The isoelectronic behaviour of these transitions is theoretically interesting, because the rates usually consist of several different contributions that grow with separate Z dependences. There

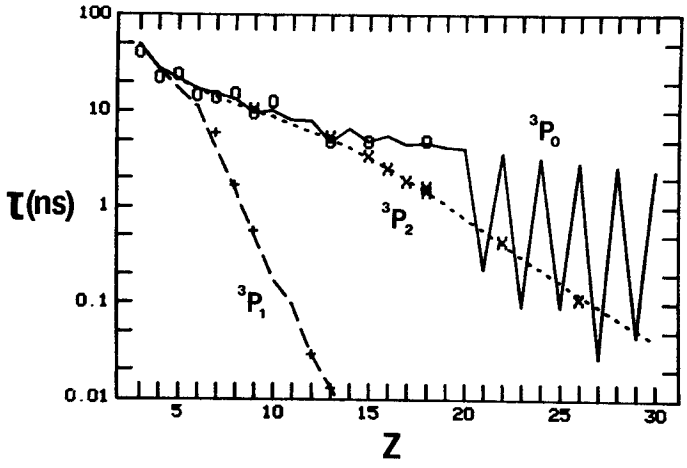

Fig. 2. Lifetime vs. atomic number for the $1s2p\ ^3P_J$ levels in the He sequence. Theoretical values are represented by a solid line for $J = 0$ [15, 16], a dotted line for $J = 2$ [15] and a dashed line for $J = 1$ [15]. Experimental measurements are represented by (○) for $J = 0$ [19, 22], by (×) for $J = 2$ [19–23] and by (+) for $J = 1$ [17–18].

has been much activity in the area recently, and a number of examples can be cited.

2.1. *The $1s2p\ ^3P_J$ levels in the He sequence*

Unlike other two-valence electron systems, the lowest ^3P state in the He sequence is not metastable, having allowed E1 transitions to the $1s2s\ ^3S_1$ level. With increasing Z, variously forbidden [14] transitions to the $1s^2\ ^1S_0$ ground state have an increasingly important effect on the lifetimes of the individual fine structure levels, as can be seen from Fig. 2 [15–23]. At low Z all three levels have similar lifetimes since the E1 transition to $1s2s\ ^3S_1$ dominates. With increasing Z the lifetime of the $^3P_1$ is drastically shortened, since the $\Delta S \neq 0$ selection rule is valid only for pure nonrelativistic LS coupling, and spin mixing causes its intercombination transition to the ground state to become E1 allowed. A similar but less drastic shortening of the $^3P_2$ lifetime takes place because of its M2 transition to ground. For systems with nonzero nuclear spin I, both the $^3P_2$ and $^3P_0$ lifetimes are affected by hyperfine-induced E1 transitions to the ground state. This is particularly striking for the $^3P_0$, because it has no other decay channel to ground, and because the effect is not smeared by a multiplicity of values of $F = I + J$. As can be seen from Fig. 2, there is a sharp "turning on" of the hyperfine quenching effect at $Z = 21$, and the alternating zero and nonzero I values in the most abundant isotopes of nuclei of even and odd Z produce a sawtooth pattern in the theoretical lifetimes [16]. Measurements for odd Z elements are not yet available for $Z > 15$, although several groups have obtained spectra for higher ions. The ratio of the $^3P_0$ to $^3P_2$ lifetimes for $Z > 20$ would provide a sensitive test of this theory.

2.2. *The $2snp\ ^3P_J$ levels in the Be sequence*

The $2s2p\ ^3P_J$ levels in the Be sequence are similar to the helium case described above, except that there are no lower-lying E1-allowed triplet decay channels so the $^3P_2$ and $^3P_0$ levels are metastable. The $^3P_1$ level has the relativistically E1-allowed intercombination transition to ground, but the excitation energy here is much lower than for a helium like ion of the same core charge, leading to a prohibitively long decay length for all but very high stages of ionisation. As shown in Fig. 1, measurements of the lifetime of this level have been made in Fe XXIII [11] and Kr XXXIII [12] which agree well with theoretical calculations [10]. Similar structures occur for the homologous $nsnp\ ^3P_J$ levels in the Mg, Zn, Cd and Hg sequences.

The $2s3p\ ^3P_J$ levels in the Be sequence are accessible to lifetime studies for much lower stages of ionisation than are the corresponding $2s2p$ levels. As in the helium case described in the previous section, this term has E1-allowed transitions to $2s3s\ ^3S_1$ and, because of its higher excitation energy, the $^3P_1$ intercombination line to ground has a sufficiently high transition probability to affect its lifetime at moderate stages of ionisation. Thus, assuming it to be the dominant cause of differences between the $^3P_{2,0}$ and $^3P_1$ lifetimes, this intercombination transition probability can be determined by differential lifetime measurements among the ^3P_J fine structure components. Such measurements have already been performed for N IV, O V and F VI [24] and for Ne VII [25]. The theoretical situation here is more complicated [26–29] than the He case described above, owing to the large number of possibilities for configuration interaction. Ellis [29] has cited this lifetime difference as an interesting test of theory, since the system is simple enough to be tractable, but the calculation must include configuration interaction, intermediate coupling and relativistic effects. Several calculations have been made which are compared with experimental values in Fig. 3.

2.3. *M1 transitions within fine structure multiplets*

Transitions between fine structure components of ground or metastable terms have come under scrutiny because of their applications in tokamak spectra [30]. Such states become heavily populated by cascades and for high Z they have large decay rates and transition wavelengths in a convenient spectral region. Examples can be found in systems with $ns^2np^x\ P$ ground state multiplets, where $x = 1$ (the doublets of the B, Al, Ga, In and Tl sequences), $x = 2$ (the triplets of the C, Si, Ge, Sn and Pb sequences), $x = 4$ (the inverted triplets of the O, S, Se, Te and Po sequences) and $x = 5$ (the inverted doublets of the F, Cl, Br, I and At sequences). Many transitions of this type have been observed in tokamak spectra, accurate extrapolations of the wavelengths have been made and multiconfiguration Hartree–Fock [32] and Dirac–Fock [10] calculations of some of the transition probabilities have been performed. Figure 1 shows the lifetimes for the 1/2–3/2 transition within the ground state

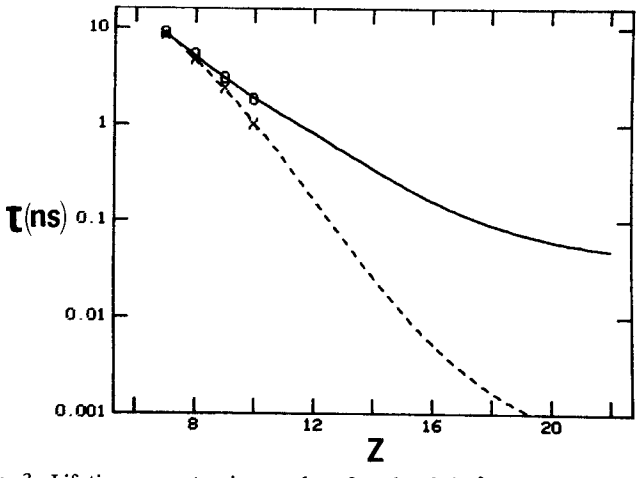

Fig. 3. Lifetime vs. atomic number for the $2s3p\ ^2P$ levels in the Be sequence. Theoretical values [27, 29] are represented by a solid line for $J = 0$ and 2, and by a dashed line for $J = 1$. Experimental measurements [24, 25] are represented by (○) for $J = 0$ and 2 and (×) for $J = 1$.

doublet of the B sequence. For some ions, the lifetimes are accessible to measurement. However, in the nonrelativistic limit of J-independent radial wave functions, M1 transition probabilities are independent of radial operators and depend only upon angular momentum considerations. Thus, the transition probability $A_{JJ'}$ from an upper state $|L,S,J\rangle$ to a lower state $|L,S,J'\rangle$ is given by [31]

$$(2J+1)A_{JJ'}(ns^{-1}) = [29.990/\lambda\,(\text{Å})]^3 S(\text{M1}) \qquad (1)$$

In nonrelativistic LS coupling the line strength S(M1) is

$$S(\text{M1}) = [(L+S+1)^2 - J_>^2]\,[J_>^2 - (L-S)^2]/4J_> \qquad (2)$$

where $J_> = \max(J,J')$. Thus, with this assumption of a constant S(M1), the lifetimes of these states are specified by the transition wavelengths alone. We have made semiempirically parametrised extrapolations of these wavelengths to high stages of ionisation for the ^2P ground states of the B and F sequences [33] and the Al, Cl, Ga, Br, In, I, Tl and At sequences [34], as well as for ^3P metastable states in the Mg sequence [35]. Perhaps not surprisingly, the use of these wavelengths in eqs. (1) and (2) yields, to within a few percent, the same results as the MCHF [32] and DF [10] calculations. Thus it seems that a lifetime measurement here would primarily test LS coupling, similar to a magnetic field quantum beat measurement of the deviation of the level g-factors from the Landé values.

2.4. *Cancellation effects*

In addition to the smooth isoelectronic variations brought about by the dependence upon nuclear charge of forbidden or inhibited transition probabilities, rapid changes restricted to one or two ions can occur due to cancellation effects. This can cause a normally strong, low lying, E1-allowed transition to be anomalously small for a specific ion, introducing measurable lifetime anomalies.

Cancellations can occur when a spectrum restructures itself with increasing Z, causing terms belonging to the ground state complex to move downward in energy relative to other terms. These "plunging" configurations interact strongly with the terms they cross, and can introduce striking irregularities in f-value trends.

An excellent example is found in the lowest-lying resonance transition of the Al sequence, $3s^23p\,^2P$–$3s3p^2\,^2D$ (LS labelling is only identificational for heavy mixing), for which, as shown in Fig. 4, almost total cancellation occurs at Si II [36]. The cascade population buildup makes it measurable in emission, but it is weak and unsaturated in absorption. This transition is well-suited to astrophysical abundance determinations and has been utilised in the analysis of Copernicus satellite data [37, 38]. Theoretical prediction of the exact isoelectronic position of the cancellation is very sensitive to the configurations included in the calculation. The theoretical values [39] for this transition shown in Fig. 4 utilised experimental information to improve an earlier calculation [40] that had placed the cancellation closer to P III.

Weiss [41] has pointed out that this type of cancellation effect is not restricted to ions near the neutral end of an isoelectronic sequence. He cites a number of examples, including $3s^23p\,^2P$–$3s^24s\,^2S$, another resonance transition in the Al sequence, also shown in Fig. 4. Here a sharp dip in the lifetime is predicted for Cr XII.

Cancellations also occur quite commonly in single configuration alkali spectra. These can be understood and predicted

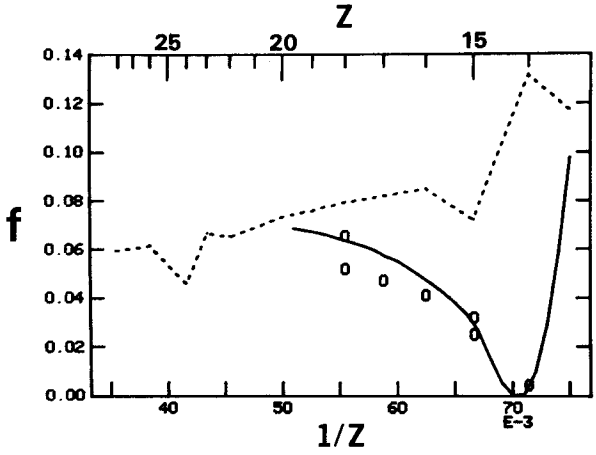

Fig. 4. Oscillator strength vs. reciprocal nuclear charge for two resonance transitions in the Al isoelectronic sequence. The solid theoretical curve [39] and the experimental measurements (cited in [39]), denoted by (o) are for the $3s^23p\,^2P$–$3s3p^2\,^2D$ transition. The dashed theoretical curve [41] is for the $3s^23p\,^2P$–$3s^24s\,^2S$ transition.

quite easily [42] in the quantum defect picture. Since the quantum defect represents a phase shift in a hydrogenic wave function in the core-external region, the isoelectronic variation of quantum defects causes a differential movement of the nodes in the upper and lower radial wave functions, leading to cancellations in the transition integral.

Such cancellations usually affect branching ratios more severely than lifetimes, since they tend to occur for wave functions with many nodes (hence many decay branches) and f sum rules redistribute the transition probabilities. The branching ratio cancellations can indirectly affect lifetime measurements; e.g., it has been observed [43] that the $4s$–$4p$ copperlike resonance transition in Kr VIII has virtually no cascading from the $5d$ level because of a cancellation [44] of the $4p$–$4d$ transition matrix for that ion. It is possible to test theoretical predictions for the ion in which a cancellation occurs by qualitatively observing the transition intensity isoelectronically, locating the ion for which it is absent. The type of "disappearance" spectroscopy was recently used [45] to locate a predicted cancellation [44] of the $4d$–$5f$ transition in the Cu sequence in Sr X.

3. Multiply excited states

Beam-foil excitation provides a light source with a profuse population of core-excited and multiply-excited configurations in highly charged ions [46], and makes possible the isoelectronic study of these systems. These states can be depopulated by autoionisation to an adjacent continuum, or by radiative deexcitation to other multiply excited states, or to the much lower-lying singly-excited states. Lifetimes measurements of these states are valuable since they reveal competition between radiative and autoionising processes, and can test methods for their theoretical calculation. These rates are important in assessing both radiation losses and dielectronic recombination (reverse autoionisation) in high temperature plasmas. A number of interesting measurements have recently been made.

3.1. *The $1s2p^2\,^4P_J$ levels in the Li sequence*

The lifetimes of quartet levels in three electron systems have been investigated extensively both experimentally and theoretically because they represent the simplest case for which the

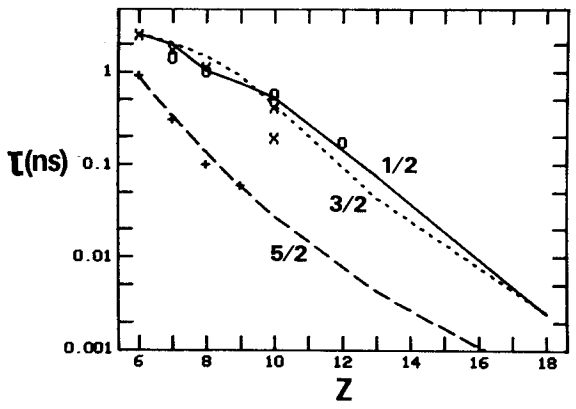

Fig. 5. Lifetime vs. nuclear charge for the individual fine structure components of the $1s2p^2\ ^4P$ decay. Experimental points (○) $J = 1/2$; (×) $J = 3/2$; and (+) $J = 5/2$ are from [47–51]. Theoretical curves, solid for $J = 1/2$; dotted for $J = 3/2$; and dashed for $J = 5/2$ are from [52].

spin multiplicity differs from that of the singly-excited states. They are metastable both to Coulomb autoionisation and to E1 transitions to the single-excited states, and the lifetimes of the fine structure components are very sensitive to the spin–orbit, spin–spin and spin–other–orbit interactions. Techniques that permit high wavelength resolution in the same optical configuration that is used for high time resolution have made possible the determination of lifetimes of the individual fine structure components of the even parity $1s2p^2\ ^4P_J$ levels in the Li sequence. These components exhibit a "differential metastability" in which a weak mixing of the $^4P_{5/2}$ level with the rapidly autoionising $^2D_{5/2}$ state of the same configuration causes its lifetime to be substantially shortened relative to the $^4P_{1/2}$ and $^4P_{3/2}$. Figure 5 displays measurements for C IV, N V and O VI [47], F VII [49], Ne VIII [48, 50] and Mg X [51], together with calculations of Chen et al. [52]. These calculations include relativistic intermediate coupling with configuration interaction, and are in closer agreement with experiment than were earlier nonrelativistic calculations [53]. Notice that for the $^4P_{1/2}$ lifetime in Ne VIII, a very recent measurement [50] removes an earlier apparent discrepancy [48].

3.2. *The $1s2p^3\ ^5S_2$ level in the Be sequence*

The $1s2s2p^2\ ^5P_J$–$1s2p^3\ ^5S_2$ transitions in the Be sequence are at present unique in that isoelectronic radiative lifetime studies have been made of them that include a negative ion. In 1980, Bunge [54] suggested that the 3489 Å line in published beam-foil spectra was due to this transition in the Li^- ion, and his suggestion was quickly verified [55–57]. This was the first time that observed line radiation was ascribed to a negative ion, but a number of other systems where this may also occur have been suggested [58, 59]. Lifetime measurements of this level for positive ions in the same sequence have also been made [49, 60], revealing interesting isoelectronic features. For example, the Li^- ion possesses only these two bound states, and, correspondingly, its decay curve is observed to be a single exponential with no cascades. For Be I–F VI [49, 60], the decay curves contain more than one exponential, indicating cascading from higher quintet states. Cascade lifetimes have been reported [49, 60], although they have not been attributed to a specific state. In addition, the measured lifetimes [60] for the positive ions are in reasonable agreement with theory [60], but the measured Li^- lifetime is 2.28(5) ns [60], significantly shorter than the calculation by Bunge [54] of 2.86(10) ns. This discrepancy is probably due to an additional decay mode involving radiative autoionisation [61] (simultaneous emission of a photon and an electron), and a calculation of this process by Nicolaides et al. [62] reduces the discrepancy by one-half.

4. Heavily cascaded levels

Much attention has been given to the problem of cascade repopulation in the analysis of decay curves [43, 63–68]. Because of the nonselective nature of the excitation process, decay curves consist of a sum of exponential contributions associated with the primary level and every level that cascades either directly or indirectly into it. The primary lifetime can be extracted by multiexponential fitting if the cascade contributions are relatively small and have lifetimes which differ substantially from that of the primary. These conditions are fulfilled for metastable forbidden or inhibited transitions, but there are many situations in which cascades preclude the reliable use of simple exponential curve fitting methods. In such cases, more powerful methods involving the joint analysis of cascade-correlated decay curves are available.

4.1. *Resonance transitions in alkali isoelectronic sequences*

The $ns\ ^2S$–$np\ ^2P$ resonance transitions of the isoelectronic sequences of alkali-like ions produce probably the most difficult of all decay curves to analyse by curve-fitting methods. These levels have only a $\Delta n = 0$ decay channel, and isoelectronically they become increasingly shorter-lived than the levels immediately above them. They are also repopulated by longer-lived high n states through cataracts [43] and cascades along the yrast chain. Thus the decay curves are affected both by fast "growing-in" and slow "growing-out" cascades, and have an "S" shape which cannot be reliably fitted without additional information. Simulations of these curves with model populations have been made for the Na [43, 63] and Cu [43, 64] isoelectronic sequences, which convincingly demonstrate that a number of early beam-foil measurements reported values that overestimated the true lifetimes by much more than the quoted uncertainties. It was clear [63] that the difficulties were of an experimental nature because, at least for highly charged ions, this particular type of transition must be considered as one of the easiest to reliably calculate. Improved experimental techniques, such as the ANDC method, that incorporate more measurements into the analysis and contain self-consistency checks, were required. Recent lifetime determinations [8, 65] utilising the correlated analysis of decay curve (ANDC) method are in excellent agreement with theoretical calculations [66].

4.2. *The ANDC method*

The ANDC method [67, 68] is simply a use of the rate equation relating the population $N_n(t)$ of the nth level to that of other levels through the transition probabilities A_{jk} and the lifetime τ_n.

$$dN_n/dt = \sum_{i>n} N_i(t)A_{in} - N_n(t)/\tau_n \qquad (3)$$

The equation can be rewritten in terms of measured decay curves $I_{jk}(t)$ since

$$I_{jk}(t) = N_j(t)A_{jk}E_{jk} \qquad (4)$$

where E_{jk} is the detection efficiency. With eq. (4), the population equation becomes a set of relationships between a given

time point t on the primary decay curve and corresponding points on its direct cascades,

$$\tau_n \, dI_{nf}/dt = \sum_{i>n} \xi_{in} I_{in}(t) - I_{nf}(t) \qquad (5)$$

with constant coefficients given by τ_n and a parameter ξ_{in} for each direct cascade (formed from products and ratios of A's and E's). Analysis consists of utilising this equation to relate measured $I(t)$'s, either by numerical differentiation or numerical integration, to determine the ξ's and τ_n through a linear regression. If all significant direct cascades have been included, the goodness-of-fit will be uniform for all subregions of t in eq. (3). If important cascades have been omitted or blends are present, this will be reflected in a variation of the goodness-of-fit in subregions of t. Very rugged algorithms have been developed [69, 70] which enable reliable lifetimes to be extracted, even in cases where the cascade contributions are overwhelmingly dominant, and studies of the propagation and correlation of errors have been made [71].

The use of this method has resolved the discrepancies between curve-fitted values and theoretical calculations in alkali sequences. In the Cu sequence the Kr VIII case has been examined in great detail, both in the simulation of decay curves [64], and in the extensive measurement of the decay curves of the $4s$–$4p$ resonance transition and all of its significant cascades [8, 65]. The ANDC analysis of [8] yielded lifetimes $\tau(^2P_{1/2}) = 291(2)$ ps and $\tau(^2P_{3/2}) = 243(10)$ ps, which compare to the theoretical values 295 and 242 ps, obtained from f value calculations by Froese-Fischer [66]. This verifies both the reliability of the calculations, and the tractability of these heavily cascaded systems to ANDC analysis. An ANDC analysis [72] has also been made for Zn II in this sequence, but there is a greater spread of results among various theoretical approaches near the neutral end of the sequence. The homologous Na-like $3s$–$3p$ transition in Fe XIV was recently studied [73] by both this method and exponential fitting, and here again the ANDC method yielded a shorter lifetime.

The ANDC method is most easily applied to systems for which repopulation effects are dominated by a small number (preferable one or two) of cascade channels. Alkali-like ns–np resonance transitions are often dominantly repopulated by cascading along the yrast chain, which is channelled entirely through the decay curve of the nearest d level. This is true for the Li, Na and Cu sequences, but for the K sequence the isoelectronic downward restructuring of the $3d$ level diverts the repopulation from the yrast chain away from the $4p$ level. This may partially explain why an ANDC analysis of the $4p$ level including only the $4d$ and $5s$ cascades was successful for Ca II [74], whereas a similar analysis for Ti IV [75] indicated that significant cascading had been omitted. Thus an ANDC analysis can actually be improved by the opening of an additional strong cascade channel, since it renders other omitted channels less important in the total repopulation. This is illustrated in a simulated example in Fig. 6. The simulation consists of a primary level and three direct cascades, with relative lifetimes 1 : 2 : 3 : 4 and relative initial populations 1 : 1 : 1 : 500. Cascades 2 and 3 are unbranched, and the heavily-populated cascade 4 is considered in two cases, with branching ratio to the primary either 0 or 1. Neither case is amenable to exponential fitting. With no branching from level 4, one-cascade ANDC analysis omitting either cascade 3 or 2 fails, as indicated by the variation of fitted lifetime as a function of t in the dotted and dashed curves. With full branching from level 4, a one-cascade ANDC analysis omitting both cascades 2 and 3 recovers the primary lifetime for all values of t except the peak of the growing-in curve, where the vanishing derivative produces a cusp.

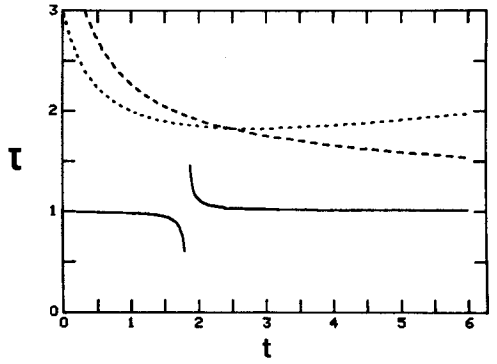

Fig. 6. ANDC lifetime vs. time since excitation for simulated decay curves. The dotted and dashed lines represent ANDC analyses of a doubly cascaded level with one cascade and then the other omitted from the analysis. The solid line represents the same situation, except that a very strong third cascade has been added, and both weaker cascades are omitted from the ANDC analysis.

The application of the ANDC method is by no means restricted to alkali-like systems. It was recently successfully applied to N IV and O V in the Be sequence [76], and has also been used, e.g., in the Mg and Al sequences [77, 78]. It does, however, require a detailed knowledge of the level scheme and the ability to measure the decay curves of the primary and all significant cascades under identical conditions.

5. Hyperalkalis

As described above, wavelength and lifetime studies indicate that theoretical calculations are very reliable for highly ionised members of the Li, Na and Cu isoelectronic sequences. Li and Na clearly represent alkali spectra, with a single electron outside of a closed-shell inert core. Although neutral Ni is not an inert gas, the Ni-like core of the Cu isoelectronic sequence increasingly acquires that characteristic with increasing Z. If we extrapolate this behaviour, the next high-Z closed $n = 4$ shell would correspond to ions isoelectronic to Nd. Thus "hyperalkali" spectra, with strong $5s$–$5p$ resonance lines should be expected for sufficiently highly ionised members of the 61 electron Pm isoelectronic sequence. These transitions would have a low excitation energy and high transition probability, and could lead to large radiative losses in plasma devices containing heavy metal contaminants.

Hartree–Fock calculations with first order relativistic corrections were made [79, 80] for the Pm sequence which indicated that the $5s$ becomes the ground state for $Z > 77$ and the $5p$ becomes the first excited state for $Z > 84$. Predictions for the wavelengths and lifetimes were also made [79]. Recent Dirac–Fock calculations [81] are in basic agreement with these predictions. However, experimental searches using beam-foil excitation of gold [82] and uranium [83] have failed to observe these lines. Theoretical methods are untested for any system of comparable complexity to these 61-electron ions, but their success in describing simpler alkali sequences raises interesting questions.

6. Conclusion

Many additional improvements in the precision of lifetime

measurements of highly charged ions can be expected in the near future. For example, the use of position sensitive detectors in fast ion beam studies [84, 85] should make possible the simultaneous measurement of the decay curves of several different spectral lines. This would permit the measurement of differential relative lifetimes, in much the same manner that spectral wavelengths are measured relative to known standard lines. This could bring new precision to the study of fine structure effects on lifetimes due to additional channels for intersystem transitions, hyperfine quenching, autoionisation, etc. It would also permit on-line ANDC analysis, with appropriate cascade-correlated decay curves measured and analysed simultaneously. Alternatively, a decay curve could be measured simultaneously with a decay which has a known quantum beat frequency superimposed, providing a precise internal clock [13].

Acknowledgements

I am grateful to Professors D. G. Ellis and A. E. Livingston for stimulating discussions. The work was supported by the U.S. Department of Energy, Division of Chemical Sciences, under contract number DE AS05 80ER10676.

References

1. Martinson, I., Comments At. Mol. Phys. **12**, 19 (1982).
2. Martinson, I., Nucl. Instr. Meth. **202**, 1 (1982).
3. Berry, H. G. and Hass, M., Ann. Rev. Nucl. Part. Sci. **32**, 1 (1982).
4. Sellin, I. A., Advances At. Mol. Phys. **12**, 215 (1976).
5. Träbert, E., Hellmann, H., Heckmann, P. H., Bashkin, S., Klein, H. A. and Silver, J. D., Phys. Lett. **93A**, 76 (1982).
6. Stoner Jr., J. O. and Leavitt, J. A., Appl. Phys. Lett. **18**, 368 (1971); Bergkvist, K. E., J. Opt. Soc. Am. **66**, 837 (1976); Jelley, N. A., Silver, J. D. and Armour, I. A., J. Phys. B: At. Mol. Phys. **10**, 2339 (1978).
7. Cheng, K. -T. and Kim, Y. -K., At. Data Nucl. Data Tables **22**, 547 (1978).
8. Livingston, A. E., Curtis, L. J., Schectman, R. M. and Berry, H. G., Phys. Rev. **A21**, 771 (1980).
9. Denne, B. and Poulsen, O., Phys. Rev. **A23**, 1229 (1981).
10. Cheng, K. T., Kim, Y. -K. and Desclaux, J. P., At. Data and Nucl. Data Tables **24**, 111 (1979).
11. Dietrich, D. D., Leavitt, J. A., Bashkin, S., Conway, J. G., Gould, H., MacDonald, D., Marrus, R., Johnson, B. M. and Pegg, D. J., Phys. Rev. **A18**, 208 (1978).
12. Dietrich, D. D., Leavitt, J. A., Gould, H. and Marrus, R., Phys. Rev. **A22**, 1109 (1980).
13. Astner, G., Curtis, L. J., Liljeby, L., Mannervik, S. and Martinson, I., Z. Physik **A279**, 1 (1976).
14. Marrus, R. and Mohr, P. J., Advances At. Mol. Phys. **14**, 181 (1978).
15. Lin, C. D., Johnson, W. R. and Dalgarno, A., Phys. Rev. **A15**, 154 (1977).
16. Mohr, P. J., in Beam-Foil Spectroscopy (Edited by I. A. Sellin and D. J. Pegg), pp. 97–103. Plenum, New York (1976).
17. For refs. to earlier lifetime measurements of the $J = 1$ level, cf. Varghese, S. L., Cocke, C. L. and Curnutte, B., Phys. Rev. **A14**, 1729 (1976).
18. Armour, I. A., Silver, J. D. and Träbert, E., J. Phys. B: At. Mol. Phys. **14**, 3563 (1981).
19. For refs. to earlier lifetime measurements of the $J = 0$, 1 levels, cf. Davis, W. A. and Marrus, R., Phys. Rev. **A15**, 1963 (1977).
20. Engström, L., Jupén, C., Denne, B., Huldt, S., Weng Tai Meng, Kaijser, P., Litzén, U. and Martinson, I., J. Phys. B: At. Mol. Phys. **13**, L143 (1980).
21. Denne, B., Huldt, S., Pihl, J. and Hallin, R., Physica Scripta **22**, 45 (1980).
22. Livingston, A. E. and Hinterlong, S. J., Nucl. Instr. Meth. **202**, 103 (1982).
23. Dohmann, H. D. and Mann, R., J. Physique (Colloque) **40**, C1-218 (1979).
24. Engström, L., Denne, B., Huldt, S., Ekberg, J. O., Curtis, L. J., Veje, E. and Martinson, I., Physica Scripta **20**, 88 (1979).
25. Hardis, J. E., Curtis, L. J., Ramanujam, P. S., Livingston, A. E. and Brooks, R. L., Phys. Rev. **A27**, 257 (1983).
26. Odabasi, H., J. Opt. Soc. Am. **59**, 583 (1969).
27. Hibbert, A., J. Phys. B: At. Mol. Phys. **12**, L661 (1979).
28. Sampson, D. H., Clark, R. E. H. and Goett, S. J., Phys. Rev. **A24**, 2979 (1981).
29. Ellis, D. G., Phys. Rev. **A28**, 1223 (1983).
30. Hinnov, E., Suckewer, S., Cohen, S. and Sato, K., Phys. Rev. **A25**, 2293. (1982); Denne, B., Hinnov, E., Suckewer, S. and Cohen, S., Phys. Rev. **A28**, 206 (1983).
31. Shortley, G. H., Phys. Rev. **57**, 225 (1940); Pasternack, S., Astrophys. J. **92**, 129 (1940).
32. Froese Fischer, C. F., J. Phys. B: At. Mol. Phys. **16**, 157 (1983).
33. Curtis, L. J. and Ramanujam, P. S., Phys. Rev. **A26**, 3672 (1982).
34. Curtis, L. J. and Ramanujam, P. S., Physica Scripta **27**, 417 (1983).
35. Curtis, L. J. and Ramanujam, P. S., J. Opt. Soc. Am. **73**, 979 (1983).
36. Curtis, L. J. and Smith, W. H., Phys. Rev. **A9**, 1537 (1974).
37. Morton, D. C., Drake, J. F., Jenkins, E. B., Rogerson, J. B., Spitzer, L. and York, D., Astrophys. J. **181**, L103 (1973).
38. Rogerson, J. B., York, D. G., Drake, J. F., Jenkins, E. B., Morton, D. C. and Spitzer, L., Astrophys. J. **181**, L110 (1973).
39. Froese Fischer, C., Can. J. Phys. **54**, 740 (1976).
40. Froese Fischer, C., J. Quant. Spectrosc. Radiat. Transfer **8**, 755 (1968).
41. Weiss, A. W., in Beam-Foil Spectroscopy (Edited by Sellin, I. A. and Pegg, D. J.), pp. 51–68. Plenum Press, New York. (1976).
42. Curtis, L. J. and Ellis, D. G., J. Phys. B: Atom. Molec. Phys. **11**, L543 (1978); **13**, L431 (1980).
43. Curtis, L. J., J. Physique (Colloque) **40**, C1-139 (1979).
44. Curtis, L. J., J. Opt. Soc. Am. **71**, 566 (1981).
45. Acquista, N. and Reader, J., J. Opt. Soc. Am. **71**, 569 (1981).
46. Berry, H. G., Physica Scripta **12**, 5 (1975).
47. Livingston, A. E. and Berry, H. G., Phys. Rev. **A17**, 1966 (1978).
48. Schumann, S., Groeneveld, K. -O., Nolte, G. and Fricke, B., Z. Physik **A289**, 245 (1979).
49. Martinson, I., Denne, B., Ekberg, J. O., Engström, L., Huldt, S., Jupén, C., Litzén, U., Mannervik, S. and Trigueiros, A., Physica Scripta **27**, 201 (1983).
50. Hardis, J. E., Berry, H. G., Livingston, A. E., Curtis, L. J. and Ramanujam, P. S., Bull. Am. Phys. Soc. **28**, 790 (1983).
51. Mowat, J. R., Jones, K. W. and Johnson, B. M., Phys. Rev. **A20**, 1972 (1979).
52. Chen, M. H., Crasemann, B. and Mark, H., Phys. Rev. **A26**, 1441 (1982).
53. Bhalla, C. P., as attributed in Ref. [47].
54. Bunge, C. F., Phys. Rev. Lett. **44**, 1450 (1980); Phys. Rev. **A22**, 1 (1980).
55. Mannervik, S., Astner, G. and Kisielinski, J. Phys. B: At. Mol. Phys. **13**, L441 (1980).
56. Brooks, R. L., Hardis, J. E., Berry, H. G., Curtis, L. J., Cheng, K. T., and Ray, W., Phys. Rev. Lett. **45**, 1318 (1980).
57. Denis, A. and Désesquelles, J., J. Physique **42**, L59 (1981).
58. Bunge, C. F., Galán, M., Jáurequi, R. and Bunge, A. V., Nucl. Instr. Meth. **202**, 299 (1982).
59. Nicolaides, C. A., Komninos, Y. and Beck, D. R., Phys. Rev. **A24**, 1103 (1981).
60. Berry, H. G., Brooks, R. L., Cheng, K. T., Hardis, J. E. and Ray, W., Physica Scripta **25**, 391 (1982).
61. Nicolaides, C. A. and Beck, D. R., Phys. Rev. **A17**, 2116 (1978); Willison, J. R., Falcone, R. W., Wang, J. C., Young, J. F. and Harris, S. E., Phys. Rev. Lett. **44**, 1125 (1980); **47**, 1827 (1981).
62. Nicolaides, C. A. and Komninos, Y., Chem. Phys. Lett. **80**, 463 (1981).
63. Crossley, R. J. S., Curtis, L. J. and Froese Fischer, C., Phys. Lett. **57A**, 220 (1976).
64. Younger, S. M. and Wiese, W. L., Phys. Rev. **A17**, 1944 (1978).
65. Pinnington, E. H., Gosselin, R. N., O'Neill, J. A., Kernahan, J. A., Donnelly, K. E. and Brooks, R. L., Physica Scripta **20**, 151 (1979).
66. Froese Fischer, C., J. Phys. B; At. Mol. Phys. **10**, 1241 (1977).
67. Curtis, L. J., Berry, H. G. and Bromander, J., Phys. Lett. **34A**, 169 (1971).
68. Curtis, L. J., in Beam-Foil Spectroscopy (Edited by Bashkin, S.),

pp. 63–109. Springer, Heidelberg (1976).
69. Weckström, K., Physica Scripta **23**, 849 (1981).
70. Engström, L., Nucl. Instr. Meth. **202**, 369 (1982).
71. Pinnington, E. H. and Gosselin, R. N., J. Physique (Colloque) **40**, C1-149 (1979).
72. Martinson, I., Curtis, L. J., Huldt, S., Litzén, U., Mannervik, S. and Jelenkovic, B., Physica Scripta **19**, 17 (1979).
73. Buchet, J. P., Buchet-Poulizac, M. C., Denis, A., Désesquelles, J. and Druetta, M., Phys. Rev. **A22**, 2061 (1980).
74. Emmoth, B., Braun, M., Bromander, J. and Martinson, I., Physica Scripta **12**, 75 (1975).
75. Baudinet-Robinet, Y., Dumont, P. D., Garnir, H. P., Grevesse, N. and Biémont, E., J. Opt. Soc. Am. **70**, 464 (1980).
76. Engström, L., Denne, B., Ekberg, J. O., Jones, K. W., Jupén, C., Litzén, U., Weng Tai Meng, Trigueiros, A. and Martinson, I., Physica Scripta **24**, 551 (1981).
77. Berry, H. G., Bromander, J., Curtis, L. J. and Buchta, R., Physica Scripta **3**, 125 (1971).
78. Curtis, L. J., Martinson, I. and Buchta, R., Physica Scripta **3**, 197 (1971).
79. Curtis, L. J. and Ellis, D. G., Phys. Rev. Lett. **45**, 2099 (1980).
81. Theodosiou, C. E. and Raftopoulos, V., Phys. Rev. **A28**, 1186 (1983).
82. Johnson, B. M., Jones, K. W., Kruse, T. H., Curtis, L. J. and Ellis, D. G., Nucl. Instr. Meth. **202**, 53 (1982).
83. Johnson, B. M. and Jones, K. W., Personal communication.
84. Johnson, B. M., Jones, K. W., Gregory, D. C., Kruse, T. H. and Träbert, E., Phys. Lett. **86A**, 285 (1981).
85. Träbert, E., Jones, K. W., Johnson, B. M., Gregory, D. C. and Kruse, T. H., Phys. Lett. **87A**, 336 (1982).